Available online at www.sciencedirect.com
SCIENCE DIRECT®
Solar Energy 80 (2006) 170–176
SOLAR ENERGY
www.elsevier.com/locate/solener

Thermal-photovoltaic solar hybrid system for efficient solar energy conversion

Yu. Vorobiev [a,*], J. González-Hernández [b,1], P. Vorobiev [c], L. Bulat [d]

[a] CINVESTAV-Querétaro, Libramiento Norponiente 2000, Querétaro 76230, Queretaro, Mexico
[b] CIMAV, Miguel de Cervantes 120, Chihuahua 31109, Mexico
[c] Facultad de Ingeniería, Universidad Autónoma de Querétaro, Queretaro, Mexico
[d] St. Petersburg State University of Refrigeration and Food Engineering, St. Petersburg 191002, Russia

Received 1 November 2004; received in revised form 13 April 2005; accepted 18 April 2005
Available online 2 August 2005

Communicated by: Associate Editor Xavier Matthew

Abstract

A hybrid solar system with high temperature stage is described. The system contains a radiation concentrator, a photovoltaic solar cell and a heat engine or thermoelectric generator. Two options are discussed, one with a special PV cell construction, which uses the heat energy from the part of solar spectrum not absorbed in the semiconductor material of the cell; the other with concentration of the whole solar radiation on the PV cell working at high temperature and coupled to the high temperature stage. The possibilities of using semiconductor materials with different band gap values are analyzed, as well as of the different thermoelectric materials. The calculations made show that the proposed hybrid system could be practical and efficient.

Keywords: Photovoltaic panel; Energy flux concentrator; Heat engine; Thermoelectric generator

1. Introduction

A key problem in solar cell science and engineering is the limited efficiency of solar energy conversion by photovoltaic cells, which results from the impossibility of an efficient utilization of the wide solar spectrum with only one semiconductor material. To overcome this problem, the combinations of different materials have been considered (multi-junction cells, see Henry, 1980; Sze, 1981; Yamaguchi, 2003), as well as the concept of a special material with an intermediate band of electronic levels within the band gap (Luque and Martí, 1997, 2001). All these devices (both existing and hypothetical ones) are very sophisticated and expensive, while their efficiency is still not satisfactory. Theoretical limits of photovoltaic conversion efficiency (Landsberg and Badescu, 1998; Landsberg, 2002) for a multi-junction cell predicts an efficiency of about 90%, but in practice not even half of that value has been obtained. On the other hand, the solar energy converters using a high temperature

* Corresponding author. Tel.: +52 442 4414 916; fax: +52 442 4414 916/938.
E-mail address: vorobiev@qro.cinvestav.mx (Yu. Vorobiev).
[1] On sabbatical leave from CINVESTAV.

0038-092X/$ - see front matter © 2005 Elsevier Ltd. All rights reserved.
doi:10.1016/j.solener.2005.04.022

Nomenclature

E_g	the band gap of semiconductor material (eV)
K	the ratio of the efficiency of high temperature stage (HTS) to that of Carnot cycle
M	optimized ratio of external-to-internal resistance for thermoelectric generator
R, r	external and internal resistances of thermoelectric generator circuit (Ω)
T	temperature (K)
T_c	temperature of the cold side of HTS
T_h	temperature of the hot side of HTS
ΔT	the temperature difference between hot and cold sides of HTS
T_{room}	room temperature
T_M	the average temperature of thermoelectric generator
Z	thermoelectric figure of merit of semiconductor material (K^{-1})
Z_0	thermoelectric figure of merit of thermoelectric module (K^{-1})
α	the thermo-emf (Zeebeck) coefficient of thermoelectric material (V/K)
β	the temperature coefficient of solar cell efficiency (K^{-1})
κ	the thermal conductivity of thermoelectric material (W/K m)
ρ	the electric resistivity of thermoelectric material (Ω m)
ξ	percentage of "thermal solar radiation" corresponding to the condition $h\nu < E_g$
η	efficiency
$\eta_{totA,B}$	the total efficiency of hybrid system for cases A and B
η_0	the room temperature efficiency of solar cell
η^*	efficiency of solar cell at temperature T_h
η_0	Carnot efficiency
η_{CA}	estimated solar cell efficiency in case A
η_{therm}	efficiency of the HTS of hybrid system in case A
η_{id}	efficiency of ideal solar cell calculated after C.H. Henry

stage have promised very high efficiency (thermophotovoltaic or thermophotonic, see Swanson, 1979; Davies and Luque, 1994; Tobías and Luque, 2002), but neither one of them proved to be practical.

Here we propose and analyze another system which also contains a high temperature stage, but with a different type of converters than those mentioned above, being actually a two-stage hybrid device including photovoltaic solar cell with the energy flux concentrator combined with a heat-to-electric/mechanic energy converter. A non-traditional approach is developed based on the utilization of the "thermal part of the solar spectrum". This could be done in two ways: one, by separating of the long wave length part of the spectrum (not absorbed in a semiconductor material of the cell) with its subsequent concentration and further conversion using a heat engine or a thermoelectric generator, and the other, by operating the cell at elevated temperatures, and use a heat engine of some kind to utilize the excess heat. Our analysis shows that this hybrid system in both versions could be efficient and practical.

2. General consideration

The scheme of the hybrid system discussed is presented in Fig. 1A and B refer to the two options mentioned above. It can be seen that the two versions are very similar and contain the same basic elements (the concentrator "CONC", photovoltaic cell "PVC", High Temperature Stage "HTS", and the 2-axis Solar Tracking System "STS2"), although the type and construction of the cell (and of concentrator) could be different in the two cases. Below we discuss the working principles and possible parameters of each system.

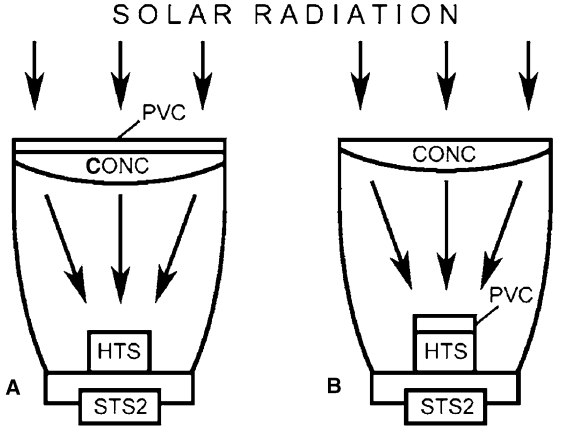

Fig. 1. Scheme of the hybrid system discussed in the text: PV cell operates at low (A) and high (B) temperatures.

2.1. System with separation of "thermal solar radiation"

It is important that in this version the photovoltaic cell operates at low (ambient) temperature (Fig. 1A). This system needs a solar cell which do not absorb or dissipate solar radiation with quantum energy $h\nu < E_g$ ("thermal solar radiation"), where E_g is the material band gap. It is shown below that this part could be quite large, especially for semiconductor materials with relatively wide band gap. Thus, in the case of a semiconductor with $E_g = 1.75$ eV, approximately 50% of solar radiation corresponds to the condition $h\nu > E_g$, and is suitable for photovoltaic conversion, and the other 50%, with $h\nu < E_g$, could be used as thermal energy. In our system, this "thermal solar radiation" is concentrated on the hot side of the HTS (thus providing its high temperature), and is converted to electric energy when HTS is a Thermoelectric Generator (TEG), or to mechanic energy by heat engine as the HTS (it could be a Stirling Engine which has efficiency very close to that of the Carnot cycle, see Organ, 1997). It is known that mechanic energy could be converted to electricity with an efficiency higher than 90% which allows having a rather high total energy conversion coefficient of the hybrid system.

To calculate the percentage of "thermal solar radiation" as a function of semiconductor band gap, we used a simple graphical analysis considering the solar spectrum, this method was first introduced by Henry (Henry, 1980) and now can be found in textbooks (Sze, 1981). This method uses a numerical integration method to determine the function $n_{ph}(E_g)$, which is the solar flux absorbed by a semiconductor, as in Henry's paper, we assume that the semiconductor is opaque for photon energies greater than E_g and transparent for energies less than E_g. This flux is given by

$$n_{ph}(E_g) = \int_{E_g}^{\infty} \frac{dn_{ph}}{d\hbar\omega} d\hbar\omega. \quad (1)$$

The obtained $n_{ph}(E_g)$ function is plotted in Fig. 2; the lower curve (squares) for AM1.5 spectrum, and the upper one (circles) for AM0. Based on these curves, and following the graphical analysis (Henry, 1980), we found the percentage ξ of "thermal solar radiation", shown by triangles in Fig. 2 (horizontal sides up for AM0, down for AM1.5, right scale). One can see that ξ varies between 10% and 12% for $E_g = 0.8$ eV and 78–80% for $E_g = 2.3$ eV.

The thermal energy part of the solar radiation has to supply the HTS (heat engine or TEG); assuming that the HTS efficiency is proportional to that of the Carnot cycle, with a coefficient $K < 1$ (the difference $K - 1$ indicates how close the HTS is to the ideal engine, i.e. $K = 1$. In general, K could be temperature dependent, in particular, in the TEG case). Thus, in this part of the solar radiation, the energy conversion is characterized by

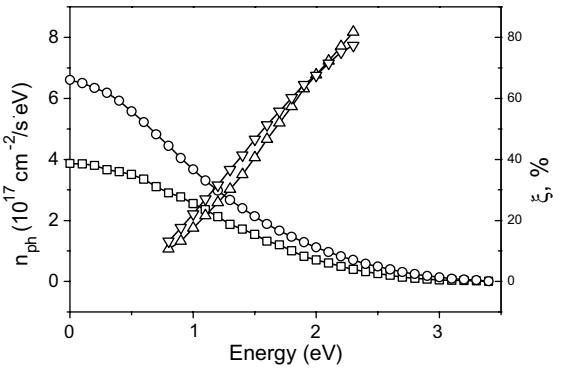

Fig. 2. Graphical analysis of the efficiency of an ideal solar cell, for AM1.5 and AM0 solar spectra (left Y-axis) and calculated percentage of "thermal" radiation (right Y-axis); for the details see text.

$$\text{Efficiency, } \eta_{therm} = \xi \cdot K\Delta T/T_h, \quad (2)$$

where T_h is the temperature of the hot side of the HTS, and ΔT the temperature difference between cold and hot sides.

The solar cells for a hybrid system of this kind have yet to be designed and made; however, we do not see any fundamental obstacles for that. To estimate the cell efficiency η_{CA} as a function of band gap, we took 0.75 of the corresponding cell's ideal efficiency η_{id} with non-concentrated radiation (Henry, 1980; Sze, 1981). Considering that for all well developed cells (based on Ge, GaAs, $CuInSe_2$) the best efficiency is well above this value, we consider this approximation is reasonable. The corresponding values ($\eta_{CA} = 0.75\eta_{id}$) for the AM1.5 irradiation are shown in Fig. 3A by squares (lower curve). The upper curve in this figure (circles) gives the total system efficiency:

$$\eta_{totA} = \eta_{CA} + \eta_{therm} = \eta_{CA} + \xi \cdot K\Delta T/T_h. \quad (3)$$

For our calculations we used $K = 0.8$ and $\Delta T = 300$ K; one could see that the total efficiency could exceed 40%.

Fig. 3B presents similar data calculated for the AM0 spectrum (cosmic conditions, non-concentrated cell illumination). Following the same graphical procedure (Henry, 1980; Sze, 1981), we calculated the ideal PV cell efficiency as a function of the band gap; the obtained values multiplied by 0.75 are shown for each E_g in Fig. 3B by squares (lower curve). The total efficiency obtained by adding η_{therm} (2) is shown by triangles (upper curve). The intermediate curves in Fig. 3A and B refer to the TEG as the HTS, and is explained.

2.2. System without the solar spectrum division, the PV cell operates at high temperature (Fig. 1B)

This system is more straightforward than the one discussed previously; the conditions for the PV cell

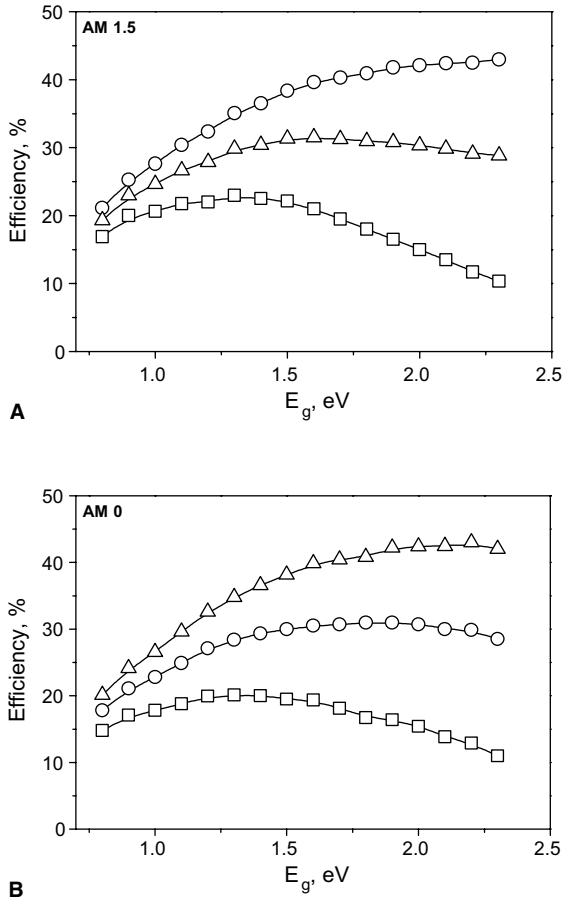

Fig. 3. (A) Calculated ideal solar cell efficiency vs. band gap × 0.75 (squares), and the total hybrid system efficiency for non-concentrated cell irradiated with AM1.5 conditions (triangles—TEG, circles—heat engine) and (B) calculated ideal solar cell efficiency vs. band gap × 0.75 (squares), and the total hybrid system efficiency for non-concentrated cell irradiated with AM0 conditions (triangles—heat engine, circles—TEG).

performance are not quite favorable here, but the system, in principle could be constructed using the elements which already exist, although the lifetime of the PV cell in question needs special study. The cell is subjected to concentrated sunlight, which usually enhances its efficiency; the thermal flux through the cell is directed into the HTS by direct thermal contact, thus the working temperature of the cell is equal to the T_h parameter of the HTS.

The limiting theoretical efficiency of an ideal system of this kind has been analyzed in the literature (Luque and Martí, 1999), with the conclusion that the efficiency is strictly equivalent to the efficiency of the photovoltaic systems, and in the limiting case in which the system involves an infinite numbers of band gaps, it will be 86.8%. Below, we present realistic estimations of the expected system efficiency. For the calculation, two types of cells with relatively high (but not the record) efficiency are considered: a GaAs single junction cell (Algora et al., 2001) with room temperature efficiency (η_0) of 24%, and multi-junction GaAs-based cell with corresponding efficiency of 30% (Yamaguchi, 2003). Both values refer to a solar radiation concentration of approximately 50 times which is sufficient to achieve the cell temperature higher than 450 K.

The temperature dependence of cell efficiency $\eta(T)$ is assumed linear with the coefficient $\beta = (d\eta/dT)/\eta$ equal to $-2.7\ 10^{-3}\ K^{-1}$ (Nann and Emery, 1992); for the temperature of 450 K the values $\eta^* = 14.3\%$ for single junction (SJ) cell, and 17.8% for multi-junction (mj) cell. Thus, practically 80% (i.e. $1 - \eta^*$) of solar radiation will be transformed into heat within the cell, and may be used for a heat-to-electric/mechanic energy conversion by the second stage of the hybrid system—a HTS. The total conversion efficiency of the hybrid system could be written as:

$$\eta_{totB} = \eta^* + (1 - \eta^*)\eta_{HTS}. \quad (4)$$

Here we have $\eta^* = \eta_0(1 - \beta\Delta T)$, $\Delta T = T_h - T_{room} \approx T_h - T_c$, ($T_c$ is the lowest temperature of the HTs which is approximately equal to the ambient temperature T_{room}), and for the HTS we consider, as in part "2A", that it is proportional to the Carnot engine efficiency: $\eta_{HTS} = K\Delta T/T_h$, this gives the expression for the total conversion efficiency:

$$\eta_{totB} = \eta_0(1 - \beta\Delta T) + [1 - \eta_0(1 - \beta\Delta T)]K\Delta T/T_h. \quad (5)$$

Fig. 4 shows the calculated results for the hybrid system with the two cells mentioned above; the temperature

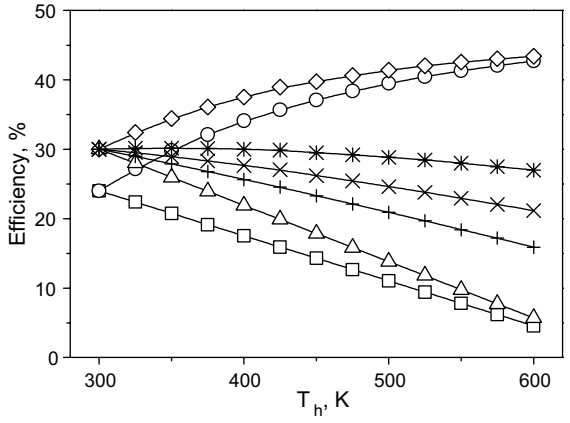

Fig. 4. Calculated temperature dependences of the PV cell efficiency (squares, triangles) and of the total hybrid system efficiency in case of the heat engine as HTS (circles, diamonds) and the TEG (three intermediate curves, $ZT = 1, 2, 4$).

dependence of the cell efficiency is shown by squares and triangles. The total efficiency is represented by the curves with circles and diamonds (circles for single junction cell, diamonds for multi-junction cell, $K = 0.8$). One could see that the second stage gives a significant boost in total efficiency for relatively modest values of ΔT, and the total efficiency could be as high as 35–40%.

3. Thermoelectric generator as a high temperature stage

The thermoelectric and photovoltaic are two direct methods for solar energy conversion, so it is natural to combine these two methods in a hybrid system. It is also important to notice that both of these methods are highly reliable and corresponding devices could work 10–30 years practically without much technical problems (see Rowe, 1995; Bulat et al., 2002) which unfortunately do not apply for heat engines.

3.1. The TEG efficiency

The efficiency of a thermoelectric generator TEG is determined by the so called thermoelectric figure of merit, Z:

$$Z = \frac{\alpha^2}{\rho\kappa}, \tag{6}$$

where ρ is the electric resistivity, κ the thermal conductivity and α the thermo-emf coefficient of the thermoelectric material (semiconductor) used. A modern thermoelectric module (a unit of a thermoelectric converter) consists of a number of alternate n- and p-type semiconductor branches connected in series (a battery). They are electrically connected in series with metallic connection strips, sandwiched between two electrically insulating and thermally conducting ceramic plates to form a module. So, any TEG contains two different materials (corresponding indexes "1" and "2"), and the optimized figure of merit for a module can be written in the form (Rowe, 1995; Bulat et al., 2002):

$$Z_0 = \frac{(\alpha_1 - \alpha_2)^2}{\left(\sqrt{\kappa_1\rho_1} + \sqrt{\kappa_2\rho_2}\right)^2}. \tag{7}$$

The efficiency of TEG can be characterized in two ways:

1. Efficiency corresponding to the classic condition of the maximum power output $R = r$ (the external electric resistance R equal to the TEG internal resistance r):

$$\eta_1 = \eta_0\left(\frac{4}{Z_0 T_h} + 2 - \frac{T_h - T_c}{2T_h}\right)^{-1}. \tag{8}$$

2. Since the thermoelectric devices (same as the photovoltaic ones) are not characterized by a constant internal resistance, there is another condition for the maximum TEG efficiency corresponding to the relation $(R/r)_{opt} = M = \sqrt{1 + Z_0 T_M}$, where T_M is the average temperature $T_M = 0.5(T_h + T_c)$. In this case:

$$\eta_{max} = \eta_0 \frac{M - 1}{M + \frac{T_c}{T_h}}. \tag{9}$$

The coefficient $\eta_0 = \frac{T_h - T_c}{T_h} = \Delta T/T_h$ in (8) and (9) is the ideal thermodynamic efficiency of a heat engine (the Carnot efficiency). Usually η_{max} is a little higher than η_1; as a rule, the difference between the values of the TEG efficiency given by the two expressions above does not exceed 4% (Rowe, 1995). Our purpose is to estimate the highest efficiency of the hybrid system, therefore we use for calculations expression (9).

3.2. Thermoelectric materials

To proceed with calculations, we have to specify a value for the figure of merit Z. It is necessary to point out that Z for semiconductors depends on temperature, and the different kinds of semiconductor materials should be selected for different operating temperatures. The commercial thermoelectric materials can be divided in the following groups depending on the operating temperature (Rowe, 1995; Bulat et al., 2002):

- for temperatures up to 500 K, solid solutions based on bismuth telluride (Bi_2Te_3, Bi_2Te_3–Bi_2Se_3);
- for temperatures up to 800 K, the PbTe;
- for space applications ($T > 900$ K), a solid solutions based on Ge–Si.

In the present days the main challenge for the thermoelectric material research is to increase Z. Despite of the efforts of many research groups in different countries, during the years 1950–2000 (Bulat et al., 2002), a marginal increase from −0.75 to 1.0 was only achieved in the room temperature value of the dimensionless thermoelectric coefficient ZT. But significant progress in the field has been made during the last few years in various aspects in this field, for instance:

(1) The use of new physical ideas in nano-scale microstructures, such as a high quality 2D quantum superlattice with nano-scale films based on p-Bi_2Te_3/Sb_2Te_3 having $ZT = 2.4$ at room temperature, obtained by Venkatasubramanian et al., 2001; Venkatasubramanian, 2001. A nanostructured material with quantum dots (1D structure) based on PbSeTe has the value of $ZT = 2.0$ at room temperature (Harman et al., 2002). The increase of the figure of merit was also obtained in a special structure with cold points (like contacts between a plate

and edge of a cone). The measured figure of merit of the last structure based on p-$Bi_{0.5}Sb_{1.5}Te_3$ and n-$Bi_2Te_{2.9}Se_{0.1}$ corresponds to $ZT = 1.7$ at room temperature (Ghoshal et al., 2002; Ghoshal, 2002).

(2) Along with semiconductor TEG there exist thermionic devices that also can be used for direct generation of electricity. However, the traditional thermionic converters work only at very high temperatures (above 800), necessary for electrons to overcome the potential barrier. But recently a new theoretical approach has been offered (Hishinuma et al., 2001) for a thermionic converter with a barrier thickness of nanometric dimensions; in this case electrons can overcome the potential barrier by quantum tunneling. Apparently such thermotunnel converter has been realized, and a $ZT = 4$ product for this thermoelectric converter was reported (Tavkhelidze et al., 2002).

(3) Another option is the application of some new bulk thermoelectric materials, for instance the so called skutterrudites and clathrates. It was shown that the thermal conductivity can be reduced in these materials (Caillat et al., 2001), therefore the figure of merit will increase. The examples of skutterrudites are $CoSb_3$ (n-type) and Zn_4Sb_3 (p-type) and of the clathrates—$CoFe_4Sb_{12}$. These materials have good figure of merit in a wide temperature range and therefore can be used for TEGs.

Thus for the calculation of the efficiency of hybrid system in the temperature range 300–600 K, we can use the following thermoelectric data: $ZT = 1$, a value found in modern industrial thermoelectrics; $ZT = 2$, reasonable value for thermoelectrics produced in laboratories (nano-scale microstructures), and $ZT = 4$, the value reported for thermionic converter with quantum tunneling.

3.3. Hybrid system with TEG

In the case of the hybrid system "A" with separation of "thermal solar radiation", we present only results for the highest ZT value (intermediate curves in Fig. 3A and B) obtained by introducing the calculated values of η_{max} (9) in expression (3) instead of the heat engine efficiency $K\Delta T/T_h$. It can be seen that in both cases (AM0 and AM1.5), for the band gap values corresponding to the most widely used PV cell materials, the total efficiency of this hybrid system with the TEG is around 30%, with an additional efficiency increase of about 5–10%, due to the TEG.

For the system "B" with PV cell operating at high temperature and having the TEG as the HTS, the calculated results for the total efficiency, using Eq. (4), and η_{max} instead of η_{HTS} for three ZT values, are shown in Fig. 4. The PV cell is assumed to be of multi-junction type, with a room temperature efficiency of 30%; the corresponding results for $ZT = 1$, 2 and 4 are shown in Fig. 4 by three descending curves starting with the efficiency of 30% at 300 K (the larger ZT, the upper curve). It is seen that the TEG has considerable effect on the efficiency in all cases.

4. Conclusion

The thermal-photovoltaic solar (TPVS) hybrid systems discussed here offer some unexplored possibilities to increase the efficiency of solar to electric energy conversion, and the analysis made could be a guide for the development of some new photovoltaic and thermoelectric devices.

References

Algora, C., Ortiz, E., Rey-Stolle, I., Dìaz, V., Peña, R., Andreev, V.M., Khvostikov, V.P., Rumyantsev, V.D., 2001. A GaAs solar cell with an efficiency of 26.2% at 1000 Suns and 25% at 2000 Suns. IEEE Trans. Electron Dev. 48, 840–844.

Bulat, L.P., Vedernikov, M.V., Vyalov, A.I., Goltsman, B.M., Drabkin, I.A., Iordanishvili, E.K., Takhistov, F.Y., Tsvetkov, O.B., 2002. in: L.P. Bulat (Ed.), Thermoelectric Cooling. St. Petersburg, SPbSUR&FE, pp. 85–147.

Caillat, T., Fleurial, J.-P., Snyder, G.J., Borschevsky, A., 2001. Development of high efficiency segmented thermoelectric uncouples. In: Proc. XX Int. Conf. on Thermoelectrics, August 8–11, IEEE, pp. 282–286.

Ghoshal, U., 2002. Design and characterisation of cold point thermoelectric coolers. In: Proc. XXI Int. Conf. on Thermoelectrics, August 26–29, IEEE, pp. 540–545.

Ghoshal, U., Ghoshal, S., McDowell, C., Shi, L., 2002. Enhanced thermoelectric cooling at cold junction interfaces. Appl. Phys. Lett. 80 (16), 3006–3008.

Harman, T.C., Taylor, P.J., Walsh, M.P., LaForge, B.E., 2002. Quantum dot superlattice thermoelectric materials and devices. Science 27 (September), 297–299.

Henry, C.H., 1980. Limiting efficencies of ideal single and multiple energy gap terrestrial solar cells. J. Appl. Phys. 51 (8), 4494–4500.

Hishinuma, Y., Geballe, T.H., Moyzhes, B.Y., Kenny, T.W., 2001. Refrigeration by combined tunneling and thermionic emission in vacuum: use of nanometer scale design. Appl. Phys. Lett. vol. 78 (17), 2572–2574.

Landsberg, P.T., Badescu, V., 1998. Solar energy conversion: list of efficiencies and some theoretical considerations. Prog. Quantum Electron. 22, 211–231.

Landsberg, P.T., 2002. Theoretical limits of photovoltaic solar energy conversion. In: Proc. of the RIO 02—World Climate and Energy Event, January 6–11, pp. 61–65.

Luque, A., Martí, A., 1997. Increasing the efficiency of ideal solar cells by photon induced transitions at intermediate levels. Phys. Rev. Lett. 78, 5014–5017.

Luque, A., Martí, A., 1999. Limiting efficiency of coupled thermal and photovoltaic converters. Sol. Energy Mater. Sol. Cells 58, 147–165.

Luque, A., Martí, A., 2001. A metallic intermediate band high efficiency solar cell. Prog. Photovoltaics 9, 73–86.

Nann, S., Emery, K., 1992. Spectral effecst on PV-device rating. Sol. Energy Mater. Sol. Cells 27, 189–216.

Organ, A.J., 1997. The Regenerator and the Stirling Engine. Harvill Press, pp. 23–26.

Rowe, D.M. (Ed.), 1995. CRC Handbook of Thermoelectrics. CRC Press, London, NY, pp. 700–702.

Sze, S.M., 1981. Physics of Semiconductor Devices, second ed. John Wiley & Sons, NY, pp. 790–838.

Swanson, R.W., 1979. A proposed thermophotovoltaic solar energy conversion system. Proc. IEEE 67, 446–447.

Tavkhelidze, A., Skhiladze, G., Bibilashvili, A., Tsakadze, L., Jangadze, L., Taliashvili, Z., Cox, I., Berishvili, Z., 2002. Thermionic converter with quantum tunneling. In: Proc. XXI Int. Conf. on Thermoelectrics, August 26–29, IEEE. pp. 435–438.

Tobías, I., Luque, A., 2002. Ideal efficiency and potential of solar thermophotovoltaic converters under optically and thermally concentrated power flux. IEEE Trans. Electron. Dev. 49, 2024–2030.

Venkatasubramanian, R., 2001. US Patent No.: 6,300,150,B1. October 9.

Venkatasubramanian, R., Silvota, E., Colpitts, T., O'Quinn, B., 2001. Thin-film thermoelectric devices with high room-temperature figures of merit. Nature 413, 597–608.

Yamaguchi, M., 2003. III–V compound multi-junction solar cells: present and future. Sol. Energy Mater. Sol. Cells 75, 261–269.